



Utilization of ^{222}Rn and Stable Isotope for Investigating Potential Tailing Storage Leaks: A Case Study from Azurite Gold Mine, Central Kalimantan

SITI ROFIKOH¹ and IRWAN ISKANDAR^{1,2}

¹Groundwater Engineering, Bandung Technology of Institute, Bandung, Indonesia

²Earth Resources Exploration Research Group, Bandung Technology of Institute, Bandung, Indonesia

Corresponding author: rofikohsiti@gmail.com

Manuscript received: December, 21, 2023; revised: July, 22, 2024;

approved: September, February, 17, 2025; available online: April, 11, 2025

Abstract - Azurite Gold Mine is an open pit project in Central Kalimantan which has produced mine tailings from the mining activities. There are various types of tailing storage facility (TSF) methods, e.g. dam tailing, landfill, and backfill to ex-mine void. Azurite Gold Mine stores their tailings in an inactive mine pit, named In-pit Seroja. The tailing placement into the inactive mine pit has less environmental impact compared to dam tailing as long as potential leakage of water-tailing into groundwater can be managed properly. The research objective is to investigate the potential tailing storage leaks into groundwater, and to determine contribution of waste dump at the northern part of In-pit tailing placement. ^{222}Rn measurements and stable isotope analyses were performed for this work. Dissolved ^{222}Rn from water samples has the concentration value between 1070 and 4940 $\text{Bq}\cdot\text{m}^{-3}$ indicating the existence of permeable zone around the In-Pit Seroja inactive mine pit. The high ^{222}Rn concentration value is coexisting with the presence of faults, especially some intersection faults. Hydrogeochemical data shows that most groundwater is included to bicarbonate type except one groundwater sample near the waste dump is the sulphate type. Based on an isotopic analysis, the ratio of $\delta^2\text{H}$ ranges from -132.55 to -6.268 ‰ for rainwater samples, -66.621 to -58.09 ‰ for groundwater samples, -97.092 to -48.43 ‰ for surface water samples, and -66.834 to -45.889 ‰ for water-tailing samples. The isotopic ratio $\delta^{18}\text{O}$ ranges from -17.795 to -2.526 ‰ for rainwater samples, -10.164 to -8.93 ‰ for groundwater samples, -13.912 to -7.714 ‰ for surface water samples, and -9.352 to -2.864 ‰ for water-tailing samples. Water-tailing has different typical stable isotope composition compared to groundwater and surface water. Heavier $\delta^{18}\text{O}$ and $\delta^2\text{H}$ ratio indicates that water-tailing has already heated by intense evaporation process. Based on hydrogeochemical and stable isotope result, combined with groundwater flow analyses, it can be concluded that there is no leakage from water-tailing into groundwater and surface water around the area.

Keywords: In-Pit TSF, water-tailing leakage, hydrogeochemical, deuterium, oxygen

© IJOG - 2025

How to cite this article:

Rofikoh, S and Iskandar, I., 2025. Utilization of ^{222}Rn and Stable Isotope for Investigating Potential Tailing Storage Leaks: A Case Study from Azurite Gold Mine, Central Kalimantan *Indonesian Journal on Geoscience*, 12 (1), p.65-74. DOI: [10.17014/ijog.12.1.65-74](https://doi.org/10.17014/ijog.12.1.65-74)

INTRODUCTION

Background

Tailing storage facility is used to manage tailing solids and mine waste that contains hazardous materials (Winarno, 2019). Azurite Gold Mine stored the mine tailings from 2021 - 2023 in their inactive mine pit, named In-Pit Seroja.

In-Pit Seroja is bounded by North Waste Dump with maximum height of 98 m at the northern part. At the western part of In-Pit Seroja lies a natural creek that flows into the Piko River with the distance of more than 1.3 km from In-Pit Seroja.

The studied area is in Dirung Village, located approximately 460 km north of Palangkaraya,

Central Kalimantan. Based on the data from rainfall gauge located 30 m from the In-Pit Seroja, the studied area has two rainfall peaks with the highest rainfall occurring in April and November. Figure 1 shows monthly rainfall data in In-Pit Seroja from 2014 - 2022. Generally, the dry season occurs from June to September, while the wet season from January to May, and October to December.

The local hydrogeological conditions at In-Pit Seroja are controlled by the east-west fault and some minor NW - SE and NE - SW faults, generating a high fracture intensity. In this paper, fracture refers to all discontinuities, such as joints, faults, cracks, bedding planes, and contacts. Fractures and fracture networks are critical conduits for the migration of water and contaminants in groundwater systems (Berkowitz, 2002). The main flow path in fractured rocks are along joints, faults, and other discontinuities (Singhal and Gupta, 1999). Due to the high fracture intensity at In-Pit Seroja which allows water from the mine tailing flow into the groundwater through the fractures, there is an increase risk of water-tailing leaks towards the groundwater.

Geochemistry and isotope methods are used to trace the origin and transformation of contaminants in groundwater, and to predict the impacts on surface waters (Clark, 2015). A stable isotope analysis was used to ascertain the water source and the mixing mechanism of groundwater (Is-

kandar and Koike, 2010). There are two main types of isotopes, namely stable isotopes and radioactive isotopes. The measure of $\delta^{2}\text{H}$ and $\delta^{18}\text{O}$ of the water molecules is the most preferred approaches to identify the groundwater flow and sources and the mechanism of pollution (Aggarwal *et al.*, 2009). Radon (^{222}Rn), a radioactive isotope, has been widely utilized in groundwater systems as a powerful tracer (Baskaran, 2016). Some of the advantages in using ^{222}Rn are that ^{222}Rn is a natural constituent of groundwater (Baskaran, 2016). As a geogenic gas, the ^{222}Rn concentration in groundwater is more significant than in surface water. When ^{222}Rn concentration in surface water become significant, it could be a sign of the presence of permeable zone which allows ^{222}Rn to be released to the surface. ^{222}Rn measurement is a powerful technique for discovering permeable fractures for the deep fluid path to the surface and the path of recharged meteoric water into the deep system (Iskandar *et al.*, 2018). Moreover, ^{222}Rn isotope can be used as a good environmental tracer with high sensitivity for the interaction between surface water and groundwater, especially in the fractured aquifer system (Wu *et al.*, 2015).

Therefore, this research aims to (i): determine the existence of permeable zone around In-Pit Seroja, (ii) assess the possibility of leaks from the water-tailing through the groundwater, and (iii) determine the waste dump contribution to water-tailing and groundwater systems.

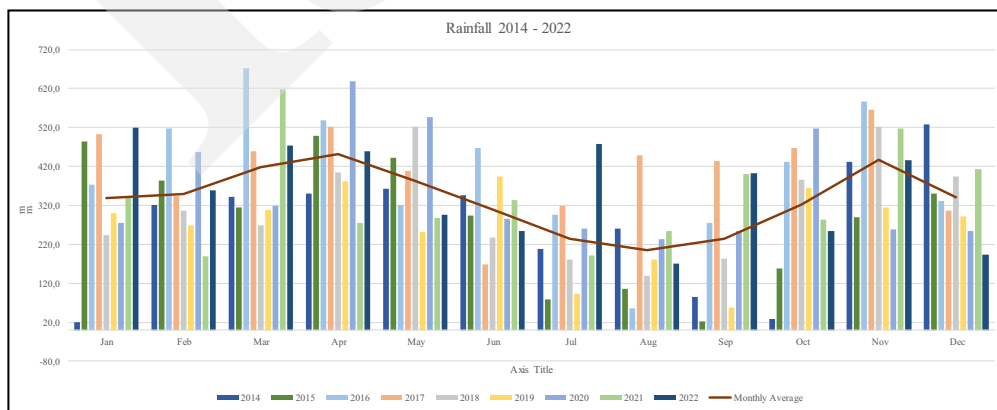


Figure 1. Monthly rainfall data from 2014 to 2022 of the studied area with two-peak rainfall intensity in April and November. Monthly amounts ranged between 55.7 - 449.2 in dry season and 258 - 639 in wet season (Source: P.T. Azurite Gold Mine, 2013).

Geological/Stratigraphical Settings

Geologically, the Azurite Gold Mine Project is located on the eastern margin of the Sundaland Continent, which is bounded by Meratus Mountains in the east and Kuching Mountains in the north (P.T. Azurite Gold Mine, 2013). The Azurite Complex is part of a northeast trending zone where discrete piles of andesitic volcanic rocks are known to occur, hosting epithermal precious metal deposits (P.T. Azurite Gold Mine, 1993).

In-pit Seroja is underlain by andesitic tuff, andesite, and basalt. Andesitic tuff is the dominant lithology observed within the pit. Locally, the rock was sheared and brecciated. The local geological setting is structurally complex, with several faulting generations of east-west dominant orientations (fault and shear zone) controlling the mineralization at In-Pit Seroja. Minor NW-SE and NE-SW faults cut earlier E-W and WNW-ESE faults.

METHODS AND MATERIALS

Field observations were conducted in this research to measure the groundwater level and to determine the local groundwater flow system at In-Pit Seroja and its surrounding areas. Dissolved ^{222}Rn concentrations were measured from ten

locations including surface water, tailing water, and groundwater using Durrige RAD-7 machine that was already calibrated.

There are 105 water samples that were collected during nine different periods (three periods in dry seasons and six in wet seasons) between June 2022 and April 2023. In more detail, there are fifteen samples were collected from rainwater, eighteen from surface water, twenty-seven from tailing water, and forty-five from groundwater wells. Samples were collected in HDPE bottles of 250 ml, afterwards the sample stored and preserved. Sample preparation and procedure are based on the sampling booklet IAEA - Sampling Procedures for Isotope Hydrology. For dissolved metals and trace elements, samples were filtered and acidified, then were analyzed in the laboratory using inductively coupled plasma-mass spectrometry Agilent Technologies 7800 ICP-MS. Major cations-anions were analyzed using ion chromatography Metrohm 930 Compact IC Flex. Isotope ratio Piccaro Civity Ringdown Spectrometer L213i-Isotopic H_2O determined the abundance of $\delta^2\text{H}$ and $\delta^{18}\text{O}$. Moreover, the materials used for the research consist of water level meter, a bailer for groundwater sampling, a plastic bottle, a membrane filter $0.2\ \mu\text{m}$, a pH meter, and 2M HNO_3 for acidifying ICP-MS samples.

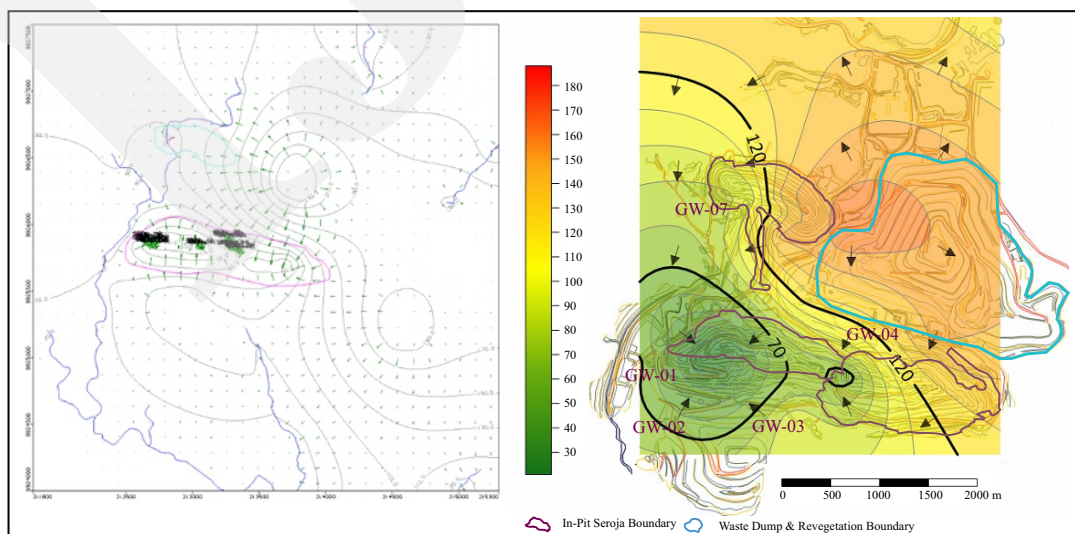


Figure 2. Groundwater flow model expresses that groundwater flows into In-Pit Seroja, as the results of inactive mine pit that has a lower hydraulic gradient than groundwater.

RESULT AND DISCUSSION

The results of groundwater flow modeling are presented in Figure 2. It can be seen that local groundwater flows from the higher elevations around In-Pit Seroja towards the In-Pit itself driven by a higher hydraulic gradient around In-Pit Seroja. The implication of this hydraulic gradient towards the pit is preventing water and contaminants from tailings spreading into the groundwater.

Dissolved ^{222}Rn measurements were carried out on surface, tailings, and groundwater samples. The average dissolved ^{222}Rn concentration varies from 0 to 4.790 Bq.m^{-3} . The values in surface and tailings water samples offer small numbers, unlike the groundwater samples. It follows the nature of ^{222}Rn as a geogenic gas, the concentration in surface was tiny. Figure 3 shows a contour map of ^{222}Rn concentration from spatial interpolation analysis. Based on the interpolation, there are four ^{222}Rn concentration zones: areas with $0 - 200 \text{ Bq.m}^{-3}$, $>200 - \leq 800 \text{ Bq.m}^{-3}$, $>800 - \leq 1800 \text{ Bq.m}^{-3}$, and $\geq 1800 \text{ Bq.m}^{-3}$.

The presence of ^{222}Rn in water can indicate the existence of a permeable zone that allows ^{222}Rn

to be released. Several factors including fracture length, aperture, intensity, and fracture intersection control the flow of water through fractures. Larger fracture lengths, greater fracture density, and larger apertures increase hydraulic conductivity (Singhal and Gupta, 1999). Therefore, for hydrogeological studies, it is extremely important to understand, to describe, and to quantify the pattern of the fractures (Golf-Racht, 1982; Sharp, 1993; Singhal and Gupta, 1999). Overlaying the geological map with ^{222}Rn concentration reveals that concentrations will be higher in zones with intense faults and veins. It is also high in areas where lithological contacts are found. The fault intensity and fault length in the researched area are presented in Table 1.

The physicochemical parameters were measured on-site during sampling, and it is shown in Table 2. Surface water that is represented by SW02 shows low TDS, whilst water-tailing has higher concentrations of dissolved solid. Surface water typically has low TDS comprising mainly dissolved inorganic ions and humic compounds derived from soils and organic molecules from in-situ biochemical processes (Clark, 2015). On

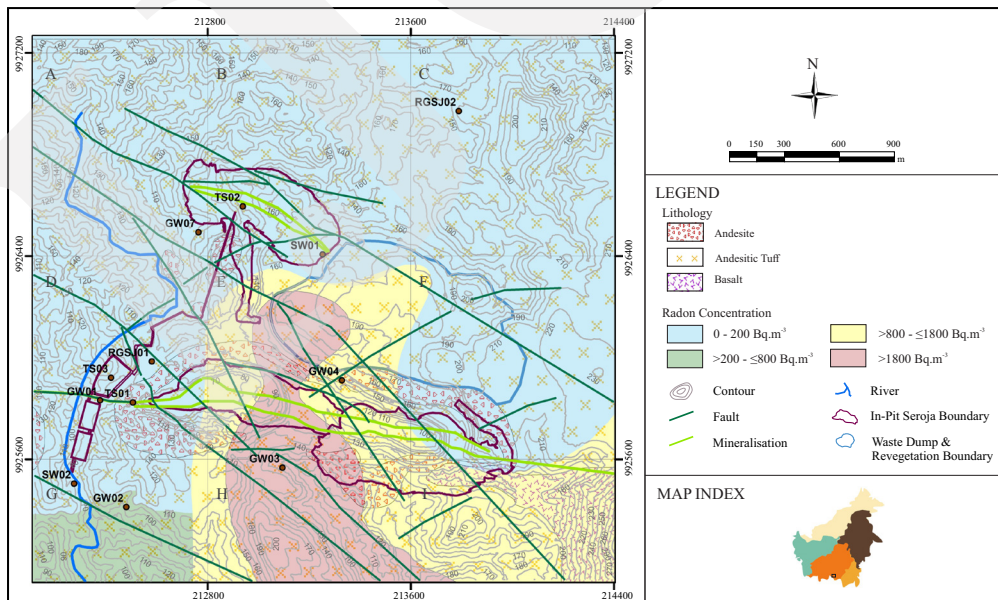


Figure 3. Geological and radon concentration map of the researched area. The ^{222}Rn concentration zone overlaid with a geological map is divided into an $800 \text{ m} \times 800 \text{ m}$ grid to calculate the fault intensity. The presence of a permeable zone at a location can be investigated using the ^{222}Rn . The higher concentration of ^{222}Rn , the more permeable it is. From the results of measuring ^{222}Rn concentration and overlaying it with a geological map, it was concluded that the middle part of In-Pit Seroja is a permeable zone characterized by a ^{222}Rn concentration of >800 to $>1800 \text{ Bq.m}^{-3}$.

Table 1. Fault Intensity and Fault Length Measured from 800 m × 800 m grid of Geological and Radon Concentration Map

Grid Area	Fracture Intensity	Fracture Length	Lithology	²²² Rn concentration
A	5	2194	Andesitic Tuff	0 - 200 Bq.m ⁻³
B	6	2293	Andesitic Tuff	0 - 200 Bq.m ⁻³
C	0	0	Andesitic Tuff	0 - 200 Bq.m ⁻³
D	8	2516	Andesitic Tuff	0 - 200 Bq.m ⁻³
E	11	4135	Andesitic Tuff - Andesite - Vein	800 - >1800 Bq.m ⁻³
F	5	1997	Andesitic Tuff - Andesite - Vein	0 - 800 Bq.m ⁻³
G	1	755	Andesitic Tuff	>200 - 800 Bq.m ⁻³
H	4	1645	Andesitic Tuff - Andesite	≥800 - >1800 Bq.m ⁻³
I	2	895	Andesitic Tuff - Andesite - Basalt	>800 - 1800 Bq.m ⁻³

(Nine grids area showed that ²²²Rn concentration will be higher in zones with intense faults, veins, and lithological contacts).

Table 2. Physicochemical Parameters of the Researched Area During Dry and Wet Seasons

Sample Code	Water Type	Period	Season	Temperature	pH	TDS	TSS
				°C		ppm	ppm
TS01	Tailing Water	Agu.22	Dry	25.2	8.52	1,778	10
		Apr.23	Wet	23.2	8.22	1,720	21
Agu.22		Dry	25.8	8.1	1,536	8	
Apr.23		Wet	23.7	8	1,450	11	
TS03		Agu.22	Dry	25.5	7.81	840	5
		Apr.23	Wet	23.3	7.92	809	15
S02	Surface Water	Agu.22	Dry	23.4	7.74	800	7
		Apr.23	Wet	25.1	7.7	726	16
GW01	Groundwater	Agu.22	Dry	25.4	8.28	218	10
		Apr.23	Wet	23.1	8.44	203	15
Agu.22		Dry	25.1	7.69	171	19	
Apr.23		Wet	22.9	7.19	165	21	
GW03		Agu.22	Dry	25.1	7.8	216	14
		Apr.23	Wet	23.1	7.56	212	35
GW04		Agu.22	Dry	27.5	8.28	372	4
		Apr.23	Wet	23.2	8.16	363	10
GW07	Agu.22	Dry	27.2	7.47	219	9	
	Apr.23	Wet	23.2	7.25	208	14	

The parameters evaluated were temperature, pH, TDS, and TSS. All samples showed neutral acidity with pH ranged from 7.19 - 8.55. TDS in the dry season ranged between 840 - 1778 ppm for water-tailing sample, 800 ppm for surface water, and 171 - 372 ppm for groundwater. Whereas the wet season ranged from 809 - 1720 ppm, 726 ppm, 165 - 363 ppm for surface water, water-tailing and groundwater respectively. TDS values were higher during the dry season.

the other hand, water-tailing has higher concentrations of dissolved inorganic ions as a result of interaction between water and tailing materials. Groundwater has a low TDS, ranging from 171 - 372 ppm in dry season, and 165 - 363 ppm in wet season. It can be indicated that groundwater flow system is not affected by water-tailing which has higher TDS.

Determination of hydrochemical facies was extensively used in the chemical assessment of groundwater and surface water for several decades (Kumar, 2012). Piper diagram (Piper,

1944) is often used to determine the main composition and hydrochemical facies of groundwater (Fenta *et al.*, 2020). Major cations and anions analyses were conducted to determine the water facies and the impact of seasonal changes on them. The results are plotted in a Piper diagram (Figure 4). It shows that rainwater samples from two rainwater gauges were in the calcium bicarbonate water facies, surface water samples (creek and waste dump channels) were in the calcium sulfate facies, and water-tailings were in sodium chloride facies. On an exciting point,

groundwater samples from monitoring wells around In-Pit Seroja show three different water facies: calcium bicarbonate, sodium bicarbonate, and sodium chloride.

Water samples around In-Pit Seroja could be grouped into four facies based on Piper diagram (Figure 3). Surface water and water-tailing samples for both wet and dry season show the dominance of $\text{Ca}^{2+} - \text{Mg}^{2+} - \text{SO}_4^{2-}$ (calcium sulfate). It indicates the presence of interaction between surface water and the wall rock that is rich in sulfides at the surface where the O_2 is present. Rainwater samples and groundwater from GW-02 and GW-07 have the same facies: calcium bicarbonate ($\text{Ca}^{2+} - \text{Mg}^{2+} - \text{HCO}_3^-$), indicating the typical of shallow groundwater is influenced by meteoric water that is CO_2 from atmosphere forms HCO_3^- . The presence of Ca^{2+} in groundwater expresses the interaction of water with igneous rocks consisting of silica and feldspar minerals. Groundwater samples from GW-01 and GW-03 belong to the sodium bicarbonate ($\text{Na}^+ - \text{HCO}_3^-$) facies. It means there was a cation exchange

process that replaced Ca^{2+} with Na^{2+} due to the silicate degradation process. Based on the water facies and low TDS value, the four groundwater samples (GW-01, GW-02, GW-03, and GW-07) are interpreted as local shallow groundwater. Shallow groundwater has a lower TDS than deeper groundwater in the same system (Freeze and Cherry, 1979).

Meanwhile, groundwater in GW-04 is sodium chloride ($\text{Na}^+ - \text{Cl}^-$) facies, interpreted as (1) a mixing process of weathering and ion exchange or (2) anthropogenic activities. Cherbotarev (1955) concluded that groundwater tended to evolve chemically toward the composition of sea water accompanied by the following regional changes in anion ($\text{HCO}_3^- \blacktriangleright \text{SO}_4^{2-} \blacktriangleright \text{Cl}^-$). These changes occur as the water moves from shallow zones of active flushing through intermediate zones into zones where the flow is very sluggish and the water is old (Cherbotarev 1955; Freeze and Cherry 1979). The saline condition caused by the enrichment of Cl triggered Na^+ to replace the previous Ca^{2+} in groundwater. Based on lower TDS value

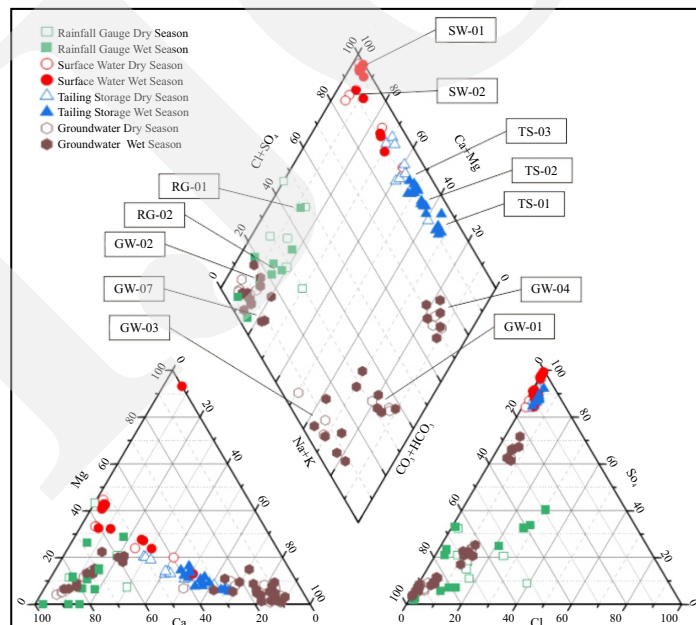


Figure 4. Piper diagram showing rainwater, surface water, water-tailing, and groundwater data for both dry and wet seasons. Rainwater sampling points are shown in green rectangle (● dry season; ● wet season), surface water in red circle (● dry season; ● wet season), water-tailing in blue triangle (● dry season; ● wet season), and groundwater in brown hexagon (● dry season; ● wet season). RG-01 and RG-02 are rainwater samples. SW-01 are surface water from north waste dump channel; SW-02 from natural creek on the southern part of In-Pit Seroja. TS-01, TS-02, and TS-03 are water-tailing samples from In-Pit Seroja (main TSF), polishing pond, and WWTP, respectively. GW-01 to GW-07 are groundwater samples.

in GW-04 samples, it can be concluded that the presence of Na⁺ and Cl⁻ are not the results of ion exchange and groundwater evolution.

The abundance of Cl⁻ in groundwater GW-04 is interpreted to originate from fertilization activities in North Waste Dump, which is a reclamation area. Sources Na⁺ - Cl⁻ in groundwater and surface water related to human activities include effluent from industrial facilities, leachate from municipal landfills, and artificial fertilizers (Panno *et al.*, 2002). Fertilizers play an important role in reclamation of degraded lands, including waste dump. Based on product description, the fertilizer used in North Waste Dump has a composition of 16 % chloride. When fertilizer is applied to the soil, rainwater infiltration dissolves chloride and leaches down into the groundwater through the permeable zone around GW-04.

Dissolved metals and REEs were obtained from the results of ICP-MS testing on surface water, water-tailings, and groundwater samples during the dry and wet seasons. Figure 5a depicts dissolved metals and trace elements for all samples. Trace elements and dissolved metals showing Cr, Fe, Zn in water-tailing samples are lower than groundwater. It can be interpreted that the source of Cr, Fe, and Zn is not coming from the water-tailing. Wall rocks in monitoring well originally contained metal which then interacted

with groundwater. Moreover, Cu, As, and Co in water-tailing samples are higher than groundwater. This is in line with natural conditions of water-tailing where the water contains Cu, As, and Co as a result of mineral extraction processes.

The measured REE concentrations are converted to a smooth curve by normalizing the REE on an element-by-element basis to one of several rock standards (Piper and Bau, 2013). Figure 5b is the REE curves of chondrite normalized profile. The anomaly of REE concentration can be seen in Figure 5b where water-tailing samples during wet season becomes very low. It is because during the wet season, volume of water-tailing increases and dilution occurs. Positive Eu anomalies occurred in all samples, but in the wet season Eu from water-tailing sample has a higher value than other REE minerals in water-tailing. Eu anomaly tends to be positive in plagioclase crystals (Varekamp, 2015). Eu has a unique chemical behaviour that makes it more incorporated into plagioclase than other minerals. When magma crystallized stable plagioclase, most of the Eu will be incorporated into the mineral causing higher Eu concentrations compared to other REE minerals (F and J., 1973). Moreover, the preferential dissolution of rock forming minerals during water and rock interaction will influence the REE pattern in the fluids. Enrichments in Na, Ca, dan Sr in the flu-

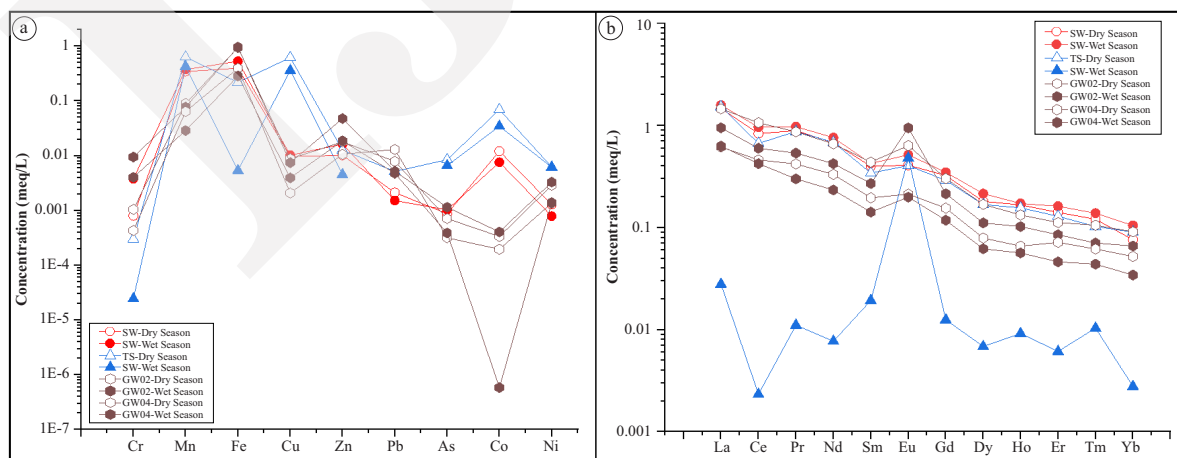


Figure 5. Trace elements and dissolved metals and REE chondrite-normalized curve: (a) Showing all dissolved metals in water-tailing are lower than groundwater except Cu, As, and Co. Groundwater samples show high concentration of Cr, Fe, and Zn for both dry and wet seasons; (b) Expresses all REE concentration in surface water, and water-tailing are higher than groundwater except in wet season. REE in water-tailing samples during the wet season becomes very low.

ids suggest plagioclase dissolution, and may be possibly associated with a positive Eu anomaly (Varekamp, 2015). Eu is resistance to remobilization during weathering and not likely to be leached out (Atwood, 2012). As the results, Eu can persist in the water-tailings for a long time.

The isotopic ratio $\delta^2\text{H}$ and $\delta^{18}\text{O}$ are plotted in a cross diagram compared with the local meteoric water line (LMWL). LMWL was constructed using local $\delta^2\text{H}$ and $\delta^{18}\text{O}$ isotope ratio of rainwater samples taken from two rainwater gauges at the researched areas (RGSJ01 and RGSJ02 sites). It can be seen in Figure 6 that the groundwater samples were plotted along the LMWL, which means the water was dominated by meteoric water. In a shallow groundwater system with normal temperature, the concentrations of $\delta^2\text{H}$ and $\delta^{18}\text{O}$ isotopes are little (Freeze and Cherry, 1979). Based on $\delta^2\text{H}$ and $\delta^{18}\text{O}$ concentration from GW-01 to GW-04, groundwater around In-Pit Seroja can be interpreted as shallow groundwater.

Creek water samples (SW02) and water-tailings (TS01, TS02, TS03) at a wet season show the $\delta^2\text{H}$ and $\delta^{18}\text{O}$ ratio shifting to the upper right indicates the water undergoes the same process: evaporation. It differs from groundwater samples where the $\delta^2\text{H}$ and $\delta^{18}\text{O}$ are plotted along LMWL. The dissimilar $\delta^2\text{H}$ and $\delta^{18}\text{O}$ isotope ratios in the groundwater and water-tailing samples can be concluded that there is no leakage from water-tailing into groundwater. Besides that, there is an anomaly of isotopic ratio from water-tailing samples in dry season where the concentration of $\delta^2\text{H}$ and $\delta^{18}\text{O}$ are close to the LMWL. It shows that there is an influx of groundwater into water-tailing system. This conclusion is also supported by the

groundwater level around In-Pit Seroja which is higher than the water-tailing level.

A simplified depiction of the hydrogeochemical conditions in the In-Pit Sertoja area is presented in Figure 7. The presence of geological structure has the potential to create permeable zones and conduits, facilitating the leakage of tailing water into groundwater system. However, in the case of In-Pit Seroja, analyses of physicochemical, hydrogeochemical, and isotopic ratio of $\delta^2\text{H}$ and $\delta^{18}\text{O}$ show different composition between water-tailing and groundwater. These differences indicate that there is no leakage from water-tailing In-Pit Seroja into groundwater.

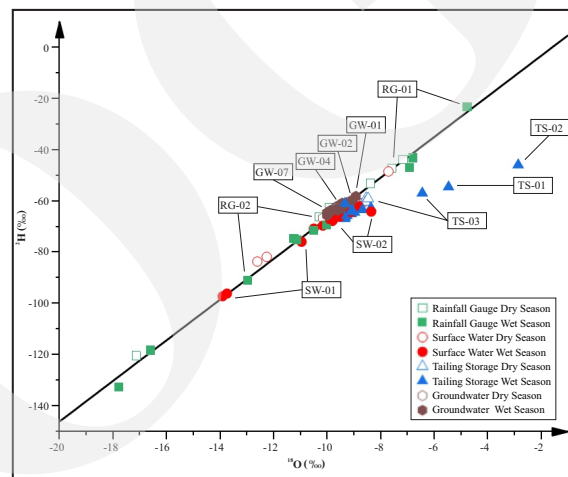


Figure 6. Cross plot diagram of $\delta^2\text{H}$ and $\delta^{18}\text{O}$ in the researched area. Based on isotopic ratio analysis, ratio of $\delta^2\text{H}$ ranges from -132.55 to -6.268 ‰ for rainwater samples, -66.621 to -58.09 ‰ for groundwater samples, -97.092 to -48.43 ‰ for surface water samples, and -66.834 to -45.889 ‰ for water-tailing samples. Isotopic ratio $\delta^{18}\text{O}$ ranges from -17.795 to -2.526 ‰ for rainwater samples, -10.164 to -8.93 ‰ for groundwater samples, -13.912 to -7.714 ‰ for surface water samples, and -9.352 to -2.864 ‰ for water-tailing samples. Some parts of the surface water and water-tailing showing evaporation process.

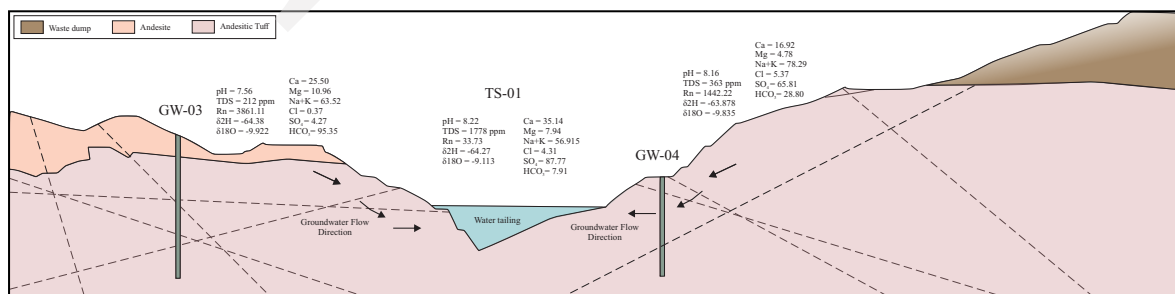


Figure 7. A simplified overview of the hydrogeochemical conditions in the In-Pit Seroja.

CONCLUSIONS

Fractures and faults play a critical role in contaminant transport study, because it can enhance the permeability of rocks. By understanding the relationship between fracture and groundwater contamination, engineers can develop more effective strategies for preventing contaminated groundwater.

Based on ^{222}Rn activity, it can be concluded that there is a permeable zone in the middle part of In-Pit Seroja which is characterized by a ^{222}Rn concentration value between >800 and >1800 $\text{Bq}\cdot\text{m}^{-3}$. The abundance of ^{222}Rn concentration is related to the intensity and length of fracture, lithological contacts, and vein system. The permeable zone becomes a conduit for the migration of groundwater into water-tailing systems.

Physicochemical, hydrogeochemical data, and isotopic ratio of $\delta^2\text{H}$ and $\delta^{18}\text{O}$ show different composition between water-tailing and groundwater which indicates that there is no leakage from water-tailing In-Pit Seroja into groundwater. Moreover, Cr, Fe, and Zn in water-tailing samples are lower than groundwater. This indicated that the source of Cr, Fe, and Zn did not come from the water-tailing. This is in line with the concentration of Cu, As, and Co as a result of mineral extraction processes in water-tailing samples which are higher than groundwater.

The analytical method using ^{222}Rn , stable isotopes $\delta^2\text{H}$ and $\delta^{18}\text{O}$, and hydrogeochemical data is quite reliable for analyzing the origin of water and the potential distribution of contaminants.

ACKNOWLEDGEMENT

The authors gratefully acknowledge the invaluable contributors of Irwan Iskandar, Rusmawan Suwarman and Musti'atin for their expertise and assistance throughout this research. We would also like to express our sincere appreciation to PT Indo Muro Kencana for allowing the authors to conduct the research. We acknowledge the crucial field support from PT IMK Staff, Anggi

Simanullang and Luthfi Luthansyah, as well as the FTTM ITB hydrogeology and hydrogeochemistry laboratory team, particularly Isel and Nita. Sincere gratitude is also extended to the anonymous reviewers and the editor-in-chief for their insightful feedback which significantly improved the quality of this paper.

REFERENCES

- Aggarwal, P. K., Froehlich, K., and Kulkarni, K.M., 2009. Environmental Isotopes in Groundwater Studies. *Groundwater*, II.
- Atwood, D.A., 2012. *The Rare Earth Elements: Fundamentals and Applications*. United Kingdom. John Willey & Sons, 629pp.
- Baskaran, M. 2016. *Radon: A Tracer for Geological, Geophysical and Geochemical Studies*. Switzerland. Springer International Publishing, 260pp. DOI: 10.1007/978-3-319-21329-3
- Berkowitz, B., 2002. Characterizing flow and transport in fractured geological media: A review. *Advances in Water Resources*. Elsevier Science *Advances in Water Resources*, 25 (8-12), p.861-884. DOI: 0.1016/S0309-1708(02)00042-8
- Cherbotarev, I.I., 1955. Metamorphism of Natural Waters in The Crust of Weathering-1. *Geochimica et Cosmochimica Acta*, 8 (1-12), p.22-48. Pergamon Press Ltd.
- Clark, I., 2015. *Groundwater Geochemistry and Isotopes*. Boca Raton. CRC Press Taylor & Francis Group, 456pp. DOI: 10.1201/b18347
- Fenta, M.C., Anteneh, Z.L., Szanyi, J., and Walker, D., 2020. Hydrogeological framework of the volcanic aquifers and groundwater quality in Dangila Town and surrounding area, Northwest Ethiopia. *Groundwater for Sustainable Development*, 11, 100408. Elsevier. DOI: 10.1016/j.gsd.2020.100408.
- Freeze, R.A. and Cherry, J.A. 1979. *Groundwater*. Prantice Hall, Inc. New Jersey, 604pp.
- Golf-Racht, 1982. *Fundamentals of Fractured Reservoir Engineering*, 1st ed., 12.

- Iskandar, I. and Koike, K., 2010. Distinguishing Potential Sources of Arsenic Released to Groundwater Around a Fault Zone Containing a Mine Site. *Research gate: Environmental Earth Science*. DOI: 10.1007/s12665-010-0727-8.
- Iskandar, I., Dermawan, F. A., Sianipar, J. Y., Suryantini, N., and Notosiswoyo, S., 2018. Characteristic and Mixing Mechanisms of Thermal Fluid at the Tampomas Volcano, West Java, Using Hydrogeochemistry, Stable Isotope and ^{222}Rn Analyses. *Geosciences*, 8 (4), 103. DOI: 10.3390/geosciences8040103.
- Kumar, P.J.S. 2013. Interpretation of Groundwater Chemistry Using Piper and Chadha's Diagrams: A Comparative Study from Perambalur Taluk. *Elixir Geoscience*, 54, p.12208-12211.
- Panno, S., Hackley, K., Hwang, H., and Greenberg, S., 2002. Source Identification of Sodium and Chloride Contamination in Natural Waters: Preliminary Results. *Research gate*. <https://www.researchgate.net/publication/260226824>.
- Piper, A.M., 1944. A graphic procedure in the chemical interpretation of water analysis. *Transaction of American Geophysical Union*, 25, p.914-928. DOI: 10.1029/TR025i006p00914.
- Piper, D.Z. and Bau, M., 2013. Normalized Rare Earth Elements in Water, Sediments, and Wine: Identifying Sources and Environmental Redox Conditions. *American Journal of Analytical Chemistry*, 4 (10A), p.69-83. DOI: 10.4236/ajac.2013.410A1009
- P.T. Azurite Gold Mine, 1993. Geological and Pit Geotechnical Investigation and Design Study. Unpublished report.
- P.T. Azurite Gold Mine, 2013. Seroja Structural Geology, Grade Distribution and New Resource Envelope. Unpublished report.
- Sharp, J.M., Jr., 1993. Fractured aquifers/reservoirs: Approaches, problems, and opportunities. In: Banks, D. and Banks, S, (eds.), *Hydrology of Hard Rocks, Memoir of the 24th Congress, International Association of Hydrologist*, 24 (1), p.23-38.
- Singhal, B.B.S. and Gupta, R.P., 1999. *Applied Hydrogeology of Fractured Rocks*. Springer-Science Business Media, B.V., 400pp.
- Varekamp, J.C., 2015. *The Chemical Composition and Evolution of Volcanic Lakes*. Springer-Verlag. DOI: 10.1007/978-3-642-36833-2_4.
- Winarno, T., Ali, R.K., and Mursalin, M., 2019. Analisis Sistem Penyaliran Tambang pada Tailing Storage Facility (TSF) PT. Aneka Tambang Tbk. Pongkor, Kabupaten Bogor, Jawa Barat. *Jurnal Geosains dan Teknologi*, 2 (3), p.135-142. DOI: 10.14710/jgt.2.3.2019.135-142
- Wu, Y., Wen, X., Zhang, Y., 2015. Analysis of The Exchange of Groundwater and River Water by Using Radon-222 in The Middle Heihe Basin of Northwestern China. *Researchgate: Environmental Earth Science*. <https://www.researchgate.net/publication/225570208>.